Author Manuscript

Author Manuscript

Author Manuscript

Author Manuscript

HHS Public Access

Author manuscript

Nat Med. Author manuscript; available in PMC 2015 May 01.

Published in final edited form as:

Nat Med. 2014 November ; 20(11): 1263–1269. doi:10.1038/nm.3699.

Niclosamide ethanolamine improves blood glycemic control and reduces hepatic steatosis in mice

Hanlin Tao[1], **Yong Zhang**[1], **Xiangang Zeng**[1,2], **Gerald I. Shulman**[3], and **Shengkan Jin**[1,*]

[1] Department of Pharmacology, Rutgers University-Robert Wood Johnson Medical School, Piscataway, NJ 08854, USA

[2] Zhejiang Key Laboratory of Applied Enzymology, Yangtze Delta Region Research Institute of Tsinghua University, Jiaxing, Zhejiang 314006, China

[3] Howard Hughes Medical Institute, Departments of Internal Medicine and Cellular & Molecular Physiology, Yale School of Medicine, New Haven, CT 06520, USA

Abstract

Type 2 diabetes (T2D) has reached an epidemic level globally. Most current treatments ameliorate the hyperglycemic symptom but are not effective in correcting the underlying cause. One important causal factor of T2D is ectopic accumulation of lipid in organs such as liver and muscle. Mitochondrial uncoupling, which reduces cellular energy efficiency and increases lipid oxidation, represents an appealing therapeutic strategy. The challenge, however, is to discover safe mitochondrial uncouplers for practical use. Niclosamide is an FDA approved anthelmintic drug that uncouples mitochondria of parasitic worms. Here we show that niclosamide ethanolamine salt (NEN) uncouples mammalian mitochondria at upper nanomolar concentrations. Oral NEN increases energy expenditure and lipid metabolism in mice. It is efficacious in preventing and treating high-fat diet (HFD) induced hepatic steatosis and insulin resistance. Moreover, it improves glycemic control and delays disease progression of the *db/db* mice. Given the well-documented safety profile of NEN, our study provides a potentially practical pharmacological embodiment of a new strategy for treating T2D.

INTRODUCTION

T2D, characterized by high plasma glucose levels and insulin resistance, has become a major medical challenge in US and around the world.[1,2] If untreated, severe and sometimes fatal complications can rapidly develop. Most patients rely on pharmacotherapy for hyperglycemic control for the rest of their lives.[3,4] However, the current available drugs are

Users may view, print, copy, and download text and data-mine the content in such documents, for the purposes of academic research, subject always to the full Conditions of use:http://www.nature.com/authors/editorial_policies/license.html#terms

*Corresponding author: victor.jin@rutgers.edu 675 Hoes Lane Piscataway, NJ 08854 Tel: 732-235-4329 Fax: 732-235-4073.

Author Contributions

H.T. and S.J. designed the experiments, analyzed the data, and wrote the manuscript. H.T. conducted most of the experiments. Y. Z. conducted the mitochondrial oxygen consumption assay, contributed to the quantitative PCR analyses and other *in vivo* studies. X.Z. contributed to the discussion and design of some experiments. G.I.S designed and supervised the analyses of hepatic lipid metabolites, and contributed to revision of the manuscript. S.J. conceived and directed the project.

Author Manuscript Author Manuscript Author Manuscript Author Manuscript

not effective in correcting the underlying cause of insulin resistance of peripheral tissues, and patients often become refractory to treatment.[3,4] Development of new anti-diabetic drugs with novel mechanisms of action, in particular those targeting the cause of insulin resistance, is important for improving diabetes therapy.

Obesity is one of the most important risk factors of T2D. Excessive accumulation of lipids affects the normal functions of adipose, liver, muscle, and pancreatic β-cells, which all contribute to the development of insulin resistance and hyperglycemia.[5-8] Although exactly how lipid accumulation leads to peripheral insulin resistance is still not fully understood, a number of mechanisms have been proposed, including increase of intracellular lipid metabolites,[9-13] inflammation and alterations in plasma cytokines.[14-20] Consistent with an important causal role of ectopic accumulation of lipid in insulin resistance, in a number of non-pharmacological approaches where T2D conditions can be effectively reversed, such as in aerobic exercise and moderate weight loss,[21-23] reversal of insulin resistance is highly correlative with a reduction of triglyceride content in liver.[24] Therefore, reducing ectopic lipid accumulation in liver or muscles is an appealing strategy for treating T2D.

Mitochondria are at the center of glucose and fatty acid metabolism. Mitochondrial uncouplers, which reduce proton gradient across mitochondrial inner membrane, create a futile cycle of glucose and fatty acid oxidation without generating ATP.[25-28] They are expected to increase lipid oxidation and reduce intracellular lipid content.[29,30] Transgenic mouse models that express the mitochondrial uncoupling proteins, UCPs, in liver or muscle exhibit elevated fatty acid oxidation and reduced intracellular lipid accumulation.[31-34] They show substantial resistance to weight gain induced by HFD feeding,[31,33] and are protected from HFD induced insulin resistance.[35,36]

The effect of mitochondrial uncoupling on reducing intracellular lipid accumulation prompted us to search for safe mitochondrial uncouplers and evaluate their potential use for T2D treatment. Partial mitochondrial uncoupling can be well tolerated by mammalian cells.[37-39] Moreover, mitochondrial uncouplers have been used in humans before. The best known chemical mitochondrial uncoupler is 2,4-dinitrophenol (DNP), which was an approved drug for treating obesity in 1930s.[40] It increases metabolic rate in humans, leading to effective loss of body fat. However, DNP has a narrow therapeutic index due to hyperthermia at high dosages, and was withdrawn from the market. The potential effect of DNP for treating T2D in humans was not adequately investigated at the time, however a recent study has shown that a liver-targeted derivative of DNP promotes hepatic fat oxidation, reduces hepatic steatosis and insulin resistance in HFD- fed and diabetic rats with a 50 fold increase in the therapeutic index compared to DNP.[41]

Niclosamide (5-chloro-salicyl-(2-chloro-4-nitro) anilide) is an FDA approved anthelmintic drug for treating intestinal infection of tapeworm.[42,43] The mechanism of action of the drug is to uncouple mitochondria of the parasitic worms,[42-44] and it has excellent safety profile.[42,43,45,46] Niclosamide ethanolamine (NEN) is a salt form of niclosamide, which has increased water solubility. The LD_{50} of oral NEN in mammals appears to be the same or even higher as compared to niclosamide.[45,46] Long-term oral treatment (ranging from months to over a year) with NEN at high dosages in experimental mammals such as rats and

Author Manuscript Author Manuscript Author Manuscript Author Manuscript

dogs do not show any adverse effects.[45,46] Encouraged by the excellent safety profile of NEN, we systematically investigated NEN as an oral treatment for T2D.

RESULTS

Properties of NEN in uncoupling mammalian mitochondria

The chemical structure of NEN salt is shown in Fig.1a. The hallmark of mitochondrial uncoupling is the induction of mitochondrial oxygen consumption even in the presence of F_oF_1 ATP synthase inhibitors, such as oligomycin.[25] NEN at the concentration of 1 μM induced oxygen consumption of isolated mitochondria from mouse liver in the presence of oligomycin (Fig. 1b). Moreover, at the same concentration, NEN dramatically increased oxygen consumption of live cells, in the presence or absence of oligomycin (Fig. 1c).

Further analyses showed that NEN started to reduce mitochondria membrane potential in live cells at the concentrations around 500 nM (Supplementary Fig. 1a). The effect was readily observed within 30 min (Supplementary Fig. 1b), and it was reversible (Supplementary Fig. 1c).

The effect of oral NEN on energy metabolism in mice

We performed pharmacokinetic and tissue distribution studies in mice after oral administration of NEN. A gavage of 40 $mg \cdot kg^{-1}$ of NEN led to peak plasma concentrations of ~400–900 $ng \cdot ml^{-1}$ (~1–2.5 μM) (Supplementary Fig. 2a). The half-life of NEN in mice was ~1.25 h (Supplementary Fig.2b). NEN was primarily distributed to liver, with relative high levels of metabolite observed in the kidney, and low or negligible levels in all other tissues examined (Supplementary Fig.2c).

We then examined the metabolic effect of oral NEN *in vivo*. We fed the mice with HFD alone (control) or HFD containing 1,500 ppm NEN (equivalent of ~150 $mg \cdot kg^{-1} \cdot day^{-1}$), a dosage well below a documented no observed adverse effect level in rodents (~25,000 ppm in feed, or 1,250 $mg \cdot kg^{-1} \cdot day^{-1}$ in rat),[45,46] and performed indirect calorimetry (IDC) studies. Compared to the controls, mice fed with NEN showed a higher energy expenditure rate (Fig. 1d). In addition, they exhibited a higher oxygen consumption rate (Fig. 1e), a marginally higher carbon dioxide production rate (Fig. 1f), and a lower respiration quotient (Fig. 1g) indicative of a larger proportion of energy expenditure derived from lipid oxidation. We also analyzed the effect of NEN on body temperature and did not observe any difference between the control and NEN- treated mice (Fig. 1h).

The effect of oral NEN on HFD- induced diabetic symptoms

The effect of oral NEN on energy expenditure and lipid oxidation prompted us to determine the effect of NEN on glycemic control. First, we tested if NEN is efficacious in preventing the development of insulin resistance and hyperglycemia in a HFD- induced diabetic mouse model. We fed C57BL/6J mice with either HFD (control) or HFD containing NEN. NEN treatment prevented the elevation of fasting blood glucose and basal plasma insulin concentrations (Fig. 2a, b). In addition, the mice fed with NEN showed better insulin sensitivity than the controls, as determined by glucose tolerance assays (Fig. 2c) and insulin

Author Manuscript Author Manuscript Author Manuscript Author Manuscript

sensitivity assays (Fig. 2d). The NEN- treated mice also exhibited slightly lower levels of glycated hemoglobin than the controls (Supplementary Fig. 3a, b). Consistent with the mitochondrial uncoupling mechanism, which increases oxidation of pyruvate rather than shunting pyruvate for the formation of lactate, as complex I inhibitors do,[47,48] mice fed with NEN exhibited lower fasting blood lactate concentrations than the controls (Fig. 2e). The better glycemic control in the NEN- treated mice correlated with smaller body weight gains (Fig. 2f), which were not caused by lower food intake or poorer nutrient absorption, as determined by food intake assay (Supplementary Fig. 3c), daily fecal weight and fecal triglyceride content analyses (Supplementary Fig.3d, e).

We further tested if oral NEN is effective in reversing hyperglycemia in the mouse model after the condition has been established. We first fed the mice with HFD for four months, then either continued with HFD feeding, or switched to HFD containing NEN. The NEN treatment significantly reduced the fasting blood glucose concentrations (Fig. 2g). The basal plasma insulin concentrations in the NEN- treated mice were also lower compared to the controls (Fig. 2h). In addition, the NEN-fed mice showed better insulin sensitivity (Fig. 2i, j). Consistently, the NEN- fed mice exhibited slightly lower levels of glycated hemoglobin (Supplementary Fig. 3f. g).

The effect of oral NEN on *db/db* mice

We further examined if oral NEN is effective in improving glycemic control in the *db/db* mouse model. At the age of 5 weeks, *db/db* mice were randomized into two groups: one group fed with normal chow (control), and the other group fed with the same chow containing 1,500 ppm NEN. Throughout the treatment course, the NEN- treated mice exhibited lower blood glucose concentrations than the controls (Fig. 3a). In addition, while plasma insulin concentrations rapidly declined in the control *db/db* mice as the disease progressed[49] (Fig. 3b), the course of plasma insulin decline was slowed down significantly in the NEN- treated mice (Fig. 3b). Consistently, the glycated HbA1c levels in the NEN-treated mice were more than 2% lower than the controls after the 60-day treatment (Fig. 3c), indicating a profoundly better glycemic control in the NEN- treated *db/db* mice. Due to rapid deterioration of the disease in*db/db* mice, the average body weight of the controls at day 60 was similar to that at day 30, despite hyperphagia. Consistent with a slower disease progression, the NEN- treated mice still show some body weight gain in the same period (Fig. 3d). Again, there was no significant difference in food intake between the control and the NEN-treated mice (Fig. 3e).

The effect of oral NEN on the liver of HFD- fed mice

In search for the mechanism by which NEN improves glycemic control, we compared the organs and tissues of mice fed with either HFD alone or HFD containing NEN. Consistent with the fact that NEN is primarily enriched in liver (Supplementary Fig. 2c), the most striking difference between the two groups of mice was the size and appearance of liver (Fig. 4a, b). Other organs, except for white adipose, did not show any apparent difference in terms of mass or appearance (data not shown). Histological analyses of liver showed that while HFD induced massive hepatic steatosis (Fig. 4c, HFD), mice fed with NEN-containing HFD showed little intracellular lipid accumulation in liver (Fig. 4c, NEN Prevention), which

Author Manuscript Author Manuscript Author Manuscript Author Manuscript

was confirmed by triglyceride content quantification of liver tissue (Fig. 4d). We then determined if oral NEN could improve hepatic steatosis after the condition has been established. We first fed the mice with HFD for four months and then switched diet to HFD containing NEN. Histological analyses and lipid content quantification showed that NEN significantly reduced lipid accumulation in liver, even though the mice were still on HFD (Fig. 4c, d, NEN Reversal).

Hepatic lipid metabolites, such as diacylglycerol (DAG) and ceramide, are important mediators of insulin resistance.[50] Consistently, the cytosolic DAG concentrations in liver from NEN-treated mice were significant lower than the controls (Supplementary Fig. 4a). However, the NEN- treated mice did not show lower hepatic ceramide contents (Supplementary Fig. 4b). Low-grade inflammation, particularly that in adipose tissue, is an important contributing factor to insulin resistance. We analyzed the expression of the pro-inflammatory cytokine *Tnf*-α and *Il-6* genes in hepatic and adipose tissues, which did not show significant difference between the mice treated with HFD and those treated with HFD containing NEN (Supplementary Fig. 4c, d). The results suggest that DAG, but not ceramide or inflammation, might be important in mediating the effect of NEN.

The ultrastructure of the hepatic tissues from mice was compared by electron microscopy (EM), which showed an overall healthier morphology of mitochondria in the liver of NEN-treated mice, characterized by round or oval shape with clear intra-organelle structure (Supplementary Fig. 5a, NEN), vs. the prolonged, deformed tubular structure observed in the control mice (Supplementary Fig. 5a, HFD). The hepatic mitochondria content did not show apparent difference between the two groups under EM (Supplementary Fig. 5a), which was confirmed by real-time PCR quantification of the mitochondrial DNA (Supplementary Fig. 5b). Consistently, the expression of the transcription factor Pgc1-α, which regulates mitochondria biogenesis, did not seem to differ between the two groups (Supplementary Fig. 5c).

Hyperinsulinemic-euglycemic clamp studies of NEN effect

We performed the clamp studies on C57BL/6J mice either fed with HFD or HFD containing NEN. The studies confirmed the higher insulin sensitivity of the NEN- treated mice, reflected by a more than 50% higher clamped glucose infusion rate required to maintain a similar euglycemic state (Table 1). The higher insulin sensitivity was associated with better hepatic insulin action, higher glucose turnover rates, and marginally lower clamp hepatic glucose production (Table 1). Moreover, the NEN-treated mice exhibited higher glycogen synthesis rates (Table 1), which were further confirmed by a direct measurement of glycogen synthesis showing higher rates in both liver and muscle (data not shown). The NEN- treated mice also contained smaller fat mass (Supplementary Table 1a), although glucose uptake by fat did not directly contribute to the improvement in insulin action (data not shown).

In addition, the clamp studies showed that the whole body glycolysis rate and the basal hepatic glucose production did not differ significantly between the two groups of mice (Table 1). This was consistent with the analyses of the glucogenogenesis enzymes, showing no significant changes in the expression of phosphoenolpyruvate carboxykinase and

Author Manuscript Author Manuscript Author Manuscript Author Manuscript

Glucose-6-phosphatase, and only a slightly lower expression of pyruvate carboxylase in the NEN-treated mice (Supplementary Fig. 6).

The effect of NEN on cellular metabolism

The *in vivo* results support the hypothesis that NEN sensitizes insulin response through uncoupling hepatic mitochondria, increasing hepatic lipid oxidation, and consequently reducing lipid accumulation in liver and likely other tissues. To examine the molecular mechanism by which NEN promotes lipid oxidation, we first characterized the effect of NEN on cellular metabolism in cultured cells. Similar to the mitochondria uncoupler DNP,[51] NEN treatment decreased cellular ATP concentration (Fig. 5a, left) and increased ADP/ATP ratio (Fig. 5a, right). Moreover, NEN activated AMPK in a dose- and time- dependent manner (Fig. 5b) that correlated with its mitochondrial uncoupling activity (Supplementary Fig. 1). In addition, NEN led to an increase in acetyl-CoA carboxylase (ACC) phosphorylation, which was at least partially dependent on AMPK activity, as treatment with an AMPK inhibitor, Compound C,[52,53] diminished ACC phosphorylation (Fig. 5c). In human liver carcinoma HepG2 cells, NEN increased fatty acid oxidation by 5-fold, which was accompanied by an activation of AMPK and an increase in phosphorylated ACC levels (Fig. 5d). These results support that in cultured cells NEN could increase lipid oxidation through activating AMPK, which phosphorylates and inhibits ACC, an inhibitor of mitochondrial β-oxidation.

We then analyzed the hepatic AMPK- ACC pathway *in vivo*. Both short-term (overnight) and chronic oral NEN treatment (weeks) increased levels of phosphorylated AMPK (Fig. 5e). In addition, chronic NEN treatment led to lower total ACC (t-ACC) protein expression (Fig. 5f) and higher phosphorylated ACC (p-ACC) to t-ACC ratio (Fig. 5f). We analyzed AMPK and ACC phosphorylation in other tissues including muscles and adipose, and no change was observed (data not shown). These results again support that liver was a direct target of NEN and the hepatic AMPK-ACC pathway contributed to the effect of NEN on promoting lipid oxidation *in vivo*.

Previous studies have shown that niclosamide could also inhibit the Wnt[54-56] or Stat3[57] pathway in cultured cell models. We tested if oral NEN affects Wnt or Stat3 pathway *in vivo* at our dosage level. Direct analyses of the pathways as well as their downstream events in mouse liver samples showed no difference between the mice fed with NEN and without NEN (Supplementary Fig. 7), indicating the two pathways did not contribute to the anti-diabetic effect of NEN. As an additional proof of the importance of the mitochondrial uncoupling activity, we made a NEN derivative (Supplementary Fig. 7f) that contains a sulfonate conjugation at the 2-hydroxyl site, an essential group for mitochondrial uncoupling.[25] The compound lost mitochondrial uncoupling activity (Supplementary Fig. 7g.) and did not show any anti-hyperglycemic activity *in vivo* (data not shown).

Discussion

Niclosamide (the free base form) is an FDA approved anthelmintic drug whose mechanism of action is to uncouple parasitic mitochondria. We tested the effect of NEN, the ethanolamine salt form of niclosamide, on hepatic lipid accumulation and hyperglycemic

Author Manuscript Author Manuscript Author Manuscript Author Manuscript

conditions in mice. Our results demonstrate that NEN uncouples mammalian mitochondria with modest potency (effective at high nanomolar concentrations). When administrated orally to mice, NEN is primarily distributed to liver and has a short half-life. Oral NEN increases energy expenditure and lipid oxidation, dramatically improves hepatic steatosis, and is efficacious in preventing and treating diabetic symptoms developed in the HFD-induced obese mice. Moreover, NEN is efficacious in treating hyperglycemia in the *db/db* mice, slows down the progression of the disease, and reduces glycated HbA1C levels by over 2%. Together, this study along with a previous study[41] demonstrate that the beneficial effects of promoting mitochondrial uncoupling in liver to increase hepatic fat oxidation can be dissociated from potential toxicities, and are in support of this approach for treating hepatic steatosis, insulin resistance and obesity-related T2D.

At the tissue and organ level, our results from the pharmacokinetic studies, tissue distribution studies, histological and biochemical analyses, as well as clamp studies, support that liver is a primary target of NEN. Our results are consistent with the model that NEN improves insulin sensitivity through its direct action of mitochondrial uncoupling in liver and consequent reduction of hepatic lipid accumulation, as well as through its secondary effect on muscle and adipose. Correlated with lower hepatic lipid accumulation, liver tissues of the NEN- treated mice show lower cytosolic DAG levels and an overall healthier mitochondrial morphology. However, these mice do not show significant change in the expression of pro-inflammatory cytokines such as *Tnf-α* and *Il-6* in liver or adipose tissue. The data support that the improvement in glycemic control by NEN may results from the benefit of improved mitochondrial function and reduction in lipid metabolites such as DAG due to the reduction in hepatic lipid loads, while NEN may not be effective in reducing inflammation.

The exact molecular mechanism underlying the upregulation of hepatic lipid oxidation by mitochondrial uncoupling might be complex. We observed that NEN reduces intracellular ATP concentration, increases ADP/ATP ratio (indicative of increase in AMP levels), activates AMPK, and increases ACC phosphorylation in cells. Likewise, NEN treatment activates AMPK and increases ACC phosphorylation (inhibition of ACC activity) in mouse liver. Thus, it is likely that the AMPK-ACC pathway is involved in upregulation of lipid oxidation triggered by mitochondrial uncoupling. Activation of AMPK through inhibiting Complex I is one of the many mechanisms proposed for the anti-diabetic action of metformin (although the contribution of this mechanism at clinically relevant dosage remains debatable[58]), which is associated with increased risk of lactic acidosis.[53] In contrast, NEN increases mitochondrial oxidation and is expected to be less likely to associate with development of lactic acidosis, which is exemplified by reduction in plasma lactate levels observed in NEN- treated mice (Fig. 2e).

Niclosamide and NEN have known toxicity profiles. In humans, the oral therapeutic dosage of niclosamide is 2,000 mg·day^{-1} (or about 25 mg·kg^{-1} ·day^{-1}) in adults, and 1,000-1,500 mg·day^{-1} in children. Despite the increased water solubility, the LD_{50} of oral NEN in mammals appears to be the same or even higher than niclosamide (LD_{50} of NEN in rats is 10,000 mg·kg^{-1}) [45,46,59]. Long-term toxicology studies (over 300 days) of oral treatment shows that non-adverse effect dosage of NEN in rats is over 25,000 ppm in feed,[45,46,59]

Author Manuscript Author Manuscript Author Manuscript Author Manuscript

which is about one order of magnitude higher than the dosage we used. It is not totally clear why oral NEN has an excellent safety profile over a wide concentration range while oral DNP has a relatively narrow therapeutic index. We suspect that the answer lies in the difference in pharmacokinetic properties between NEN and DNP. The peak levels of DNP following ingestion correlate well with toxicity,[41] whereas NEN is rapidly metabolized by liver, with a half-life about 1.5 hour and no significant accumulation in body after several hours (Supplementary Fig. 2). In addition, NEN is still relatively poorly soluble in water,[45] which effectively limits the maximal absorption rate of this drug. This would serve as an additional fail-safe mechanism against possible accumulation of NEN associated with overdose. Moreover, NEN is mostly albumin-bound in plasma,[60] which limits the extraction of NEN to tissues other than liver. In particular, existing toxicology studies did not indicate that niclosamide or NEN increases body temperature. [45,46,59] This is consistent with our results that despite the fact that NEN increases energy expenditure, it does not increase body temperature (Fig. 1h). The outcome is likely due to the mild nature of mitochondrial uncoupling by NEN upon oral administration and the robustness of the body temperature homeostatic regulation in mice.

In summary, we provide evidence that NEN, a salt form of the FDA approved drug niclosamide, has excellent anti-diabetic effect. NEN represents a new class of anti-diabetic compounds with a novel mechanism of action associated with a number of appealing features. For example, it may provide a cure to hepatic insulin resistance since it improves hepatic steatosis and corrects the underlying etiologic factor, and it may not increase the risk of lactic acidosis. NEN itself has well documented safety profile in animals. This study opens the possibility of further developing NEN and other safe mitochondrial uncouplers for treating metabolic diseases.

Online Materials and Methods

Reagents

The sources of the following reagents were: Niclosamide (2′, 5′-dichloro-4′-nitrosalicylanilide), Sigma Aldrich (St. Louis, MO); Niclosamide ethanolamine salt (NEN, niclosamide 5-chloro-salicyl-(2-chloro-4-nitro) anilide 2-aminoethanol salt), 2A PharmaChem (Lisle, IL); the sulfonate conjugated niclosamide (SCN), customarily synthesized by Provid Inc. (Piscataway, NJ); Insulin (Humulin-R Insulin U-100), Eli Lilly (Indianapolis, IN); 1-^{14}C oleic acid, GE Healthcare (Piscataway, NJ). Ultra-sensitive mouse insulin ELISA kit was from Crystal Chem Inc (Downers Grove, IL). BD™ Oxygen Biosensor System was from BD Biosciences (Franklin Lakes, NJ). EnzyLight™ ADP/ATP Ratio Assay Kit (ELDT-100) was from BioAssay Systems (Hayward, CA). GHb/A1c Mice Research Test Kit was from DTI Laboratories, Inc. (Thomasville, GA). For antibodies, AMPKα mAb (#2793), Phospho-AMPKα (Thr172) mAb (#2535), Acetyl-CoA carboxylase (C83B10) antibody (#3676), Phospho-acetyl-CoA carboxylase (Ser79) antibody (#3661), Stat3 mAb (#4904) and Phospho-Stat3 (Tyr705) antibody (#9131) were from Cell Signaling Technology (Danvers, MA). Phosphoenolpyruvate carboxykinase 1 antibody (NBP1-54825), Pyruvate carboxylase antibody (NBP1-49536) and Glucose-6-phosphatase (NBP1-80533) antibody were from Novus Biologicals (Littleton, CO). β-catenin antibody

Author Manuscript Author Manuscript Author Manuscript Author Manuscript

(sc-65483), Pgc-1α antibody (sc-13067) and Ran antibody (sc-1156) were from Santa Cruz Biotechnology (Dallas, TX).

Animals and treatments

Male C57BL/6J mice or male *db/db* mice were used in the studies as indicated. 4 weeks old male C57BL/6J mice (Stock# 000664) and 4 weeks old male *db/db* mice (BKS.Cg-*Dock7*^{m} +/+ *Lepr*^{db}/J, Stock# 000642) were purchased from the Jackson Laboratory (Bar Harbor, ME). These mice were shipped to the vivarium of Rutgers-RWJMS, or of University of Massachusetts (for clamp studies), or of Case Western Reserve University (for IDC studies), where the respective animal studies were performed. All experimental protocols were approved by the Institutional Animal Care and Use Committees (IACUC) at the respective institutions. Starting at age of 5 weeks, mice were randomized into different groups, which were fed with the various types of diets. For the C57BL/6J mice, the animals were fed with either high-fat diet (HFD, 60% fat calorie, Research Diet, New Brunswick, NJ) or HFD containing 1,500 ppm NEN (mixed and prepared by Research Diet, using NEN supplied by Jin Lab). For the *db/db* mice, the animals were fed with either normal rodent chow AIN-93M (Research Diet, New Brunswick, NJ) or AIN-93M diet containing 1,500 ppm NEN (mixed and prepared by Research Diet, using NEN supplied by Jin Lab). Animal sample size for each individual study was chosen based on literature documentation of the similar well- characterized assays. The animal studies were not blinded to investigators.

Cell culture and treatment

NIH-3T3 fibroblasts or human liver carcinoma cell line HepG2 were cultured in Dulbecco's modified Eagle's medium (DMEM) supplemented with 10% (vol/vol) fetal bovine serum, 100 unit·ml^{-1} of penicillin, 100 μg·ml^{-1}of streptomycin and 0.29 mg·ml^{-1}of L-glutamine at 37°C and 5% CO_2. For treatment, NEN was first dissolved in DMSO to make stock solution, and then was added directly to the culturing medium to desired concentration by at least 1:1000 dilution.

Protein extraction and immunoblotting

Cells or tissues were collected and homogenized within lysis buffer containing 10 mM TRIS-HCl (pH 7.9), 10% glycerol, 0.1 mM EDTA, 100 mM KCl, 0.2% NP-40, 0.5 mM PMSF, 1 mM DTT, mini-complete protease inhibitor cocktail (Roche, 11836153001), and phosphatase inhibitor cocktail (Roche, 04906845001) if required. Nuclei and insoluble debris were pelleted in an Eppendorf micro-centrifuge at 10,000 rpm for 5 min at 4°C. Cell extracts were then stored at −20°C or immediately subjected to sodium dodecyl sulfate-polyacrylamide gel electrophoresis (SDS-PAGE). For the SDS-PAGE, cell extracts were mixed with 5× Laemmli loading buffer and heated at 95°C for 5 min prior to electrophoresis. For immunoblotting, proteins were transferred to polyvinylidene difluoride (PVDF) membranes (Millipore, IPVH00010). Prior to incubating with primary antibody, membranes were blocked with 5% milk in phosphate-buffered saline supplemented with 0.1% (vol/vol) Tween-20 for 1 h at room temperature. Chemiluminescent detection was completed with ECL western blotting reagents (Amersham, 95038-566). Quantification was

Author Manuscript Author Manuscript Author Manuscript Author Manuscript

determined by measuring band intensity using ImageJ software and calculating the ratio of protein of interesting to internal loading control.

Uncoupling activity assays

Mitochondrial oxygen consumption assay was performed on isolated mitochondria as previously reported.[61,62] Briefly, mitochondria were isolated from fresh mouse liver. 1.0 mg mitochondria in a volume of 1.0 ml respiration buffer (225 mM Mannitol, 75 mM sucrose, 10 mM KCl, 10 mM Tris-HCl, pH 7.2, 5 mM KH_2PO_4, pH 7.2) was analyzed for oxygen consumption in the presence of respiration substrates with a Hansatech oxygen electrode (Hansatech Instrument, Norfolk, UK). The final concentrations of the various components added into the respiration system were as follows: succinate, 5 mM; ADP, 125 nM; oligomycin, 5 μg ·ml^{-1}; NEN, 1 μM; KCN, 2 mM.

For mitochondrial uncoupling analysis with cultured cells, the NIH-3T3 cells were seeded onto 6-well plate and cultured in DMEM medium to log phase. The cells were then treated with NEN at various concentrations and for various period of time, followed by staining with TMRE (tetramethylrhodamine ethyl ester) at a final concentration of 100 nM for 10 min. The cells were then washed once with PBS, and examined under fluorescence microscopy.

The cellular oxygen consumption was measured by the BD™ Oxygen Biosensor System. The NIH-3T3 cells were cultured in DMEM medium and seeded onto the oxygen biosensor 96-well plate at a density of 20,000 cells per well. Treatment was initiated by adding NEN (1 μM) or oligomycin (5 μg·ml^{-1}), or both into the medium. Oxygen consumption (decrease in oxygen concentrations) was indicated by generation of fluorescent signal, which was initially quenched by oxygen.

Cellular ATP and ADP assay

Cellular ATP and ADP concentrations were measured by the EnzyLight™ ADP/ATP Ratio Assay Kit. HepG2 cells were cultured on 96-well white opaque microplate to a density of 10^3-10^4 cells in each well. Then cells were treated with 1 μM NEN or vehicle for 2 h, and the ATP and ADP assays were performed following the product manufacturer's manual.

Cellular β-oxidation assay

The β-oxidation rate of free fatty acid was measured as previously reported,[63] with some modifications. HepG2 cells were cultured in DMEM medium on 6-well plate to a density of 1×10^6 cells per well. For the assay, add to each well 1ml Krebs-Ringer phosphate buffer containing fatty acid-free BSA (20 mg·ml^{-1}), glucose (2.5 mM), oleic acid (0.4 mM, Sigma), and 1-^{14}C oleic acid (1.0 μCi·ml^{-1}, GE Healthcare). To start the treatment, NEN (1.0 μM) or vehicle were added into each well, which was then covered by a piece of square filter paper soaked with hyamine hydroxide (Perkin Elmer). After incubation for 3 h, 0.5 ml of 4 M H_2SO_4 was added to each well and then the wells were sealed again for additional 30 min before the filter papers were carefully removed. The $^{14}CO_2$ trapped on each filter paper was measured by a scintillation counter (Beckman LS 5000 TD Liquid Scintillation System).

Author Manuscript Author Manuscript Author Manuscript Author Manuscript

Blood glucose and plasma insulin

The mice for measuring blood glucose were kept away from diet but with free water supply for overnight (16 h, 5:00 p.m. to 9:00 a.m.), and then blood glucose concentrations were determined using OneTouch UltraSmart blood glucose monitoring system (Lifescan). For measuring plasma insulin, the mice were fasted for 5-6 h and then the blood samples of each mouse were collected from the tail vein. The insulin levels were determined by the ultra-sensitive mouse insulin ELISA kit (Crystal Chem Inc.), following manufacturer's manual.

Glucose tolerance assay and insulin sensitivity assay

For glucose tolerance test, mice were first fasted overnight (16 h), and then intraperitoneally injected with 20% glucose at a dose of 2 $g \cdot kg^{-1}$ of body weight. The blood glucose concentrations were then measured at time points 0, 15, 30, 60, 90, and 120 min after the injection of glucose. For insulin sensitivity test, mice were first fasted for 5-6 h, and then intraperitoneally injected with recombinant human insulin at a dose of 0.75 $unit \cdot kg^{-1}$of body weight. The blood glucose concentrations were then measured at time points 0, 15, 30, 60, 90, and 120 min after the insulin injection.

Glycated hemoglobin determination

The glycated hemoglobin A1c levels and glycated total hemoglobin levels of the C57BL/6J mice (n = 8) were measured by GHb/A1c Mice Research Test Kit (DTI Laboratories, Inc.). Mouse blood samples were collected from tail vein of mice fed with HFD or HFD containing 1,500 ppm NEN for 16 wk, or first fed with HFD for 16 wk, followed by 4 wk feeding with HFD containing 1,500 ppm NEN. The blood samples were sent to DTI Laboratories, Inc, which did the analyses. The glycated hemoglobin A1c levels in the *db/db* mice (n = 9) were determined by the US National Mouse Metabolic Phenotyping Center (MMPC) at University of California, Davis (UC Davis). The blood samples were collected from tail vein of mice that had been fed with normal diet or normal diet containing 1,500 ppm NEN for 60 d.

Measurement of hepatic triglyceride

For the quantification of hepatic triglyceride (TG) content, 0.2-0.3 g of freshly dissected mouse liver tissue were homogenized with 1 ml saline solution, and then total triglyceride was extracted with 20 ml solvent (chloroform/methanol, v/v 2:1). The homogenized suspensions were then filtered through Whatman filter paper, and 10 ml of clean solution were transferred to a clean vial and air-dried. The remained triglycerides were then dissolved within 5 ml solvent containing 60% butanol and 40% of the Triton-X114/ methanol mix (v/v 2:1). Final triglyceride contents were determined by the triglyceride determination kit (Sigma) and normalized to tissue weight.

Mouse liver histological analysis

For liver histological studies, mice were sacrificed by decapitation and liver tissues were fixed with neutral buffered formalin 10% (Surgipath Medical Industries, Inc.) and embedded in paraffin. Tissue sections were prepared and stained with hematoxylin and eosin (H&E). For the oil red O staining, liver tissues were prepared as frozen sections. Images were

Author Manuscript Author Manuscript Author Manuscript Author Manuscript

acquired with a Universal Microscope Axioplan 2 imaging system (Carl Zeiss) with phase contrast objectives.

Electron microscopy

Electron microscopy study of the liver tissues was performed in collaboration with the university electron microscopy core facility.[64] C57BL/6J mice were fed with HFD or HFD containing 1,500 ppm NEN for 8 weeks (n = 3). The liver tissues were then dissected and fixed with 2.5% gluteraldehyde and 4% paraformaldehyde in 0.1 M cacodylate buffer. The thin sections (90 nm) of each sample were prepared on a Reichert Ultracut E microtome. Sections were viewed with a JEOL 1200EX transmission electron microscope.

Metabolic cage studies

The Metabolic cage studies were performed by MMPC at Case Western Reserve University. C57BL/6J mice were fed with HFD or HFD containing 1,500 ppm NEN for 1 wk (n = 8). The oxygen consumption, carbon dioxide generation, energy expenditure and respiration quotient of the mice were determined by indirect calorimetry (IDC),[65] using the Oxymax system (Columbus Instruments' Comprehensive Lab Animal Monitoring System, Columbus, OH). Experiments were performed on mice in the presence of food. The data were collected every 18 min on each mouse and continued for more than 24 h (including 12 h light phase and 12 h dark phase). The results were reported as 90- min intervals (each point represents an average of five 18- min intervals). Body temperatures of the mice were measured by rectal probe.

Pharmacokinetic studies

Pharmacokinetic analyses of oral NEN in mouse were performed by BioDuro Inc. using method previously described.[66] Briefly, NEN was dissolved in 0.5% methyl cellulose and given to male C57BL/6J mice (n = 3) at age of 6 wk by gavage at the dose of 40 $mg \cdot kg^{-1}$, blood samples were collected at indicated time points. 10 μl plasma was mixed with 2 μl methanol and 200 μl of 200 $ng \cdot ml^{-1}$internal standard diclofenac in acetonitrile, kept at −20 °C for 30 min, 10 μl of supernatant after vortex and centrifuge was subjected to LC/MS/MS analyses. For tissue distribution studies, NEN was administered to mice (n=3 for each time point) by gavage at the dose of 40 $mg \cdot kg^{-1}$. Mice were then sacrificed at 2 h, 4 h, 8 h, 24 h time points. 100 mg of each tissue was homogenized with 5X volume of water (500 μl), 50 μl of the homogenate was mixed with 5 μl methanol and 300 μl of 200 $ng \cdot ml^{-1}$internal standard diclofenac in acetonitrile, kept at −20℃ for 30 minutes, and then vortex for 1 min and centrifuge at 12,000 g for 15 min. 10 μl of supernatant was subjected to LC/MS/MS analyses.

Hyperinsulinemic-euglycemic clamp study

The hyperinsulinemic-euglycemic clamp studies were performed by MMPC at University of Massachusetts as previous described.[67] Briefly, C57BL/6J mice (n = 14) were fed with HFD or HFD containing 1,500 ppm NEN for 8 weeks before the clamp studies. After an overnight fast, mice were subjected to a 2-h hyperinsulinemic-euglycemic clamp with a primed-continuous infusion of human insulin at a rate of 2.5 $mU \cdot kg^{-1} \cdot min^{-1}$ to raise plasma

Author Manuscript Author Manuscript Author Manuscript Author Manuscript

insulin within a physiological range. 20% glucose was infused at variable rates to maintain plasma glucose at basal concentrations. All infusions were performed using microdialysis pumps. Insulin-stimulated whole-body glucose turnover was estimated with a continuous infusion of [3-^{3}H] glucose throughout the clamps (0.1 μCi·min^{-1}). To estimate insulin-stimulated glucose uptake in individual tissues, 2-deoxy-D-[1-^{14}C] glucose (2-[^{14}C] DG) was administered as a bolus (10 μCi) at 75 min after the start of clamps. Blood samples were taken during and at the end of clamps for measurement of plasma [^{3}H] glucose, $^{3}H_2O$, 2-[^{14}C] DG concentrations, insulin concentrations. At the end of the clamps, mice were anesthetized with sodium pentobarbital injection. Within 5 min, three muscles (gastrocnemius, tibialis anterior, and quadriceps) from both hindlimbs, epididymal white adipose tissue, and liver were collected for biochemical analyses. 11 mice per group with a complete set of data were included and analyzed. Student t-test was used to determine the statistical significance between the control and NEN treated mouse groups.

DAG and ceramide assays

Intrahepatic DAG and ceramide analyses were performed as previously described.[68] C57BL/6J mice (n = 8) were fed with HFD or HFD containing 1,500 ppm NEN for 8 weeks, then liver tissues were dissected and frozen in liquid nitrogen immediately. For DAG and ceramide extraction, liver tissues were homogenized in a buffer solution (20 mM Tris-HCl, 1 mM EDTA, 0.25 mM EGTA, 250 mM sucrose, 2 mM PMSF) containing a protease inhibitor mixture, and samples were centrifuged at 100,000 g for 1 h. The supernatants containing the cytosolic fraction and the pellet containing the plasma membrane were collected as previously described. [68] Both the cytosolic and membrane contents of DAGs and ceramides were measured by LC/MS/MS. The contents of DAGs and ceramides are expressed as the sum of individual species including DAGs (C16:1, C16:0, C18:2, C18:1, and C18:0) and ceramides (C16:0, C18:0, C20:0, C22:0, C24:1, C24:0). All measurements were performed in animals under basal conditions following a 6-h fast.

Quantitative real-time PCR assays

For quantitative real-time PCR analyses, total RNA was extracted from mouse liver or white adipose tissue lysates by using TRIzol reagent (Invitrogen, Carlsbad, CA) using standard protocol. 5-20 ng of total RNA from each sample was then used to generate high fidelity cDNA for quantitative PCR analyses. The cDNA was amplified by using AffinityScript QPCR cDNA Synthesis Kit (Agilent Technologies, Santa Clara, CA). For mitochondrial gene Cytochrome c oxidase subunit II (*Coxii*), DNA was prepared and analyzed. The following primers were used for the Taqman real-time PCR assays:

Phosphoenolpyruvate carboxykinase (*Pepck*):

Forward, 5’-AGCGGATATGGTGGGAAC-3’;

Reverse, 5’-GGTCTCCACTCCTTGTTC-3’

Glucose-6-phosphatase (*G6pc*):

Forward, 5’-AAAGAGACTGTGGGCATCAATC-3’;

Author Manuscript Author Manuscript Author Manuscript Author Manuscript

Reverse, 5’-AATGCCTGACAAGACTCCAGCC-3’

E-Cadherin:

Forward, 5’-ACTGTGAAGGGACGGTCAAC-3’;

Reverse, 5’-GGAGCAGCAGGATCAGAATC-3’

Tumor necrosis factor alpha (*Tnf-α*):

Forward, 5’-GGCAGGTCTACTTTGGAGTCATTGC-3’;

Reverse, 5’-ACATTCGAGGCTCCAGTGAATTCGG-3’

Interleukin 6 (*Il-6*):

Forward, 5’-GAGGATACCACTCCCAACAGACC-3’;

Reverse, 5’-AAGTGCATCATCGTTGTTCATACA-3’

Cytochrome c oxidase subunit II (*Coxii*):

Forward, 5’-CTGAAGACGTCCTCCACTCA-3’;

Reverse, 5’-TCAGAGCATTGGCCATAGAA-3’

Taqman real-time PCR was done in triplicate with TaqMan PCR mixture (Applied Biosystems). The relative expression levels of each gene were normalized against the expression of *Gapdh* gene.

Statistical analysis

One-way analysis of variance (ANOVA) was used for the statistical analyses in IDC (indirect calorimetry) studies. Student's t-test was used for the statistical analyses in all other studies. Data are presented as means ± s.d. and statistical significances are denoted as * $P < 0.05$, ** $P < 0.01$, *** $P < 0.001$.

Supplementary Material

Refer to Web version on PubMed Central for supplementary material.

Acknowledgements

We thank M. Kahn of Yale University School of Medicine for the analysis of hepatocellular DAG and ceramide contents. We thank US National Mouse Metabolic Phenotyping Centers (MMPC) at various sites for the various metabolic studies: C. Croniger and L. Wang at Case Western Reserve University (U24 DK076174) for the metabolic cage experiments; J. Kim and D.Y. Jung at University of Massachusetts (U24 DK093000) for the hyperinsulinemic-euglycemic clamp studies and glycogen synthesis rate determination; S.S. Wirth and J. Graham at University of California, Davis (U24 DK092993) for determination of the glycated haemoglobin (HbA1c) in *db/db* mice. We also thank W. Hu and Y. Zhao at Rutgers University for assistance with the quantitative real-time PCR analyses, R. Patel at Rutgers Core Facility for technical assistance with electron microscopy studies.

Author Manuscript Author Manuscript Author Manuscript Author Manuscript

H. Tao, Y. Zhang, X. Zeng and S. Jin are supported by US National Institutes of Health (R01AG030081, R01CA116088) and Mito Biopharm, LLC. G.I. Shulman is supported by US National Institutes of Health (R24 DK085638, P30 DK45735, U24 DK059635) and the Novo Nordisk Foundation for Basic Metabolic Research.

References

1. Boyle JP, Thompson TJ, Gregg EW, Barker LE, Williamson DF. Projection of the year 2050 burden of diabetes in the US adult population: dynamic modeling of incidence, mortality, and prediabetes prevalence. Popul Health Metr. 2010; 8:29. [PubMed: 20969750]
2. Center for Disease Control and Prevention. 2011 National Diabetes Fact Sheet. 2011
3. Qaseem A, Humphrey LL, Sweet DE, Starkey M, Shekelle P. Oral pharmacologic treatment of type 2 diabetes mellitus: a clinical practice guideline from the American College of Physicians. Ann Intern Med. 2012; 156:218–231. [PubMed: 22312141]
4. Nathan DM, et al. Medical management of hyperglycemia in type 2 diabetes: a consensus algorithm for the initiation and adjustment of therapy: a consensus statement of the American Diabetes Association and the European Association for the Study of Diabetes. Diabetes Care. 2009; 32:193–203. [PubMed: 18945920]
5. Kahn SE, Hull RL, Utzschneider KM. Mechanisms linking obesity to insulin resistance and type 2 diabetes. Nature. 2006; 444:840–846. [PubMed: 17167471]
6. Muoio DM, Newgard CB. Obesity-related derangements in metabolic regulation. Annu Rev Biochem. 2006; 75:367–401. [PubMed: 16756496]
7. Randle PJ. Regulatory interactions between lipids and carbohydrates: the glucose fatty acid cycle after 35 years. Diabetes Metab Rev. 1998; 14:263–283. [PubMed: 10095997]
8. Samuel VT, Petersen KF, Shulman GI. Lipid-induced insulin resistance: unravelling the mechanism. Lancet. 2010; 375:2267–2277. [PubMed: 20609972]
9. An J, et al. Hepatic expression of malonyl-CoA decarboxylase reverses muscle, liver and whole-animal insulin resistance. Nat Med. 2004; 10:268–274. [PubMed: 14770177]
10. Chavez JA, Summers SA. A ceramide-centric view of insulin resistance. Cell metabolism. 2012; 15:585–594. [PubMed: 22560211]
11. Griffin ME, et al. Free fatty acid-induced insulin resistance is associated with activation of protein kinase C theta and alterations in the insulin signaling cascade. Diabetes. 1999; 48:1270–1274. [PubMed: 10342815]
12. Holland WL, et al. Inhibition of ceramide synthesis ameliorates glucocorticoid-, saturated-fat-, and obesity-induced insulin resistance. Cell metabolism. 2007; 5:167–179. [PubMed: 17339025]
13. Samuel VT, Shulman GI. Mechanisms for insulin resistance: common threads and missing links. Cell. 2012; 148:852–871. [PubMed: 22385956]
14. Zhang Y, et al. Positional cloning of the mouse obese gene and its human homologue. Nature. 1994; 372:425–432. [PubMed: 7984236]
15. Pelleymounter MA, et al. Effects of the obese gene product on body weight regulation in ob/ob mice. Science. 1995; 269:540–543. [PubMed: 7624776]
16. Uysal KT, Wiesbrock SM, Marino MW, Hotamisligil GS. Protection from obesity-induced insulin resistance in mice lacking TNF-alpha function. Nature. 1997; 389:610–614. [PubMed: 9335502]
17. Yamauchi T, et al. The fat-derived hormone adiponectin reverses insulin resistance associated with both lipoatrophy and obesity. Nat Med. 2001; 7:941–946. [PubMed: 11479627]
18. Steppan CM, et al. The hormone resistin links obesity to diabetes. Nature. 2001; 409:307–312. [PubMed: 11201732]
19. Yuan M, et al. Reversal of obesity- and diet-induced insulin resistance with salicylates or targeted disruption of Ikkbeta. Science. 2001; 293:1673–1677. [PubMed: 11533494]
20. Yang Q, et al. Serum retinol binding protein 4 contributes to insulin resistance in obesity and type 2 diabetes. Nature. 2005; 436:356–362. [PubMed: 16034410]
21. Henry RR, Wallace P, Olefsky JM. Effects of weight loss on mechanisms of hyperglycemia in obese non-insulin-dependent diabetes mellitus. Diabetes. 1986; 35:990–998. [PubMed: 3527829]

Author Manuscript Author Manuscript Author Manuscript Author Manuscript

22. Kantartzis K, et al. High cardiorespiratory fitness is an independent predictor of the reduction in liver fat during a lifestyle intervention in non-alcoholic fatty liver disease. Gut. 2009; 58:1281–1288. [PubMed: 19074179]
23. Perseghin G, et al. Increased glucose transport-phosphorylation and muscle glycogen synthesis after exercise training in insulin-resistant subjects. N Engl J Med. 1996; 335:1357–1362. [PubMed: 8857019]
24. Petersen KF, et al. Reversal of nonalcoholic hepatic steatosis, hepatic insulin resistance, and hyperglycemia by moderate weight reduction in patients with type 2 diabetes. Diabetes. 2005; 54:603–608. [PubMed: 15734833]
25. Terada H. Uncouplers of oxidative phosphorylation. Environ Health Perspect. 1990; 87:213–218. [PubMed: 2176586]
26. Nedergaard J, Ricquier D, Kozak LP. Uncoupling proteins: current status and therapeutic prospects. EMBO reports. 2005; 6:917–921. [PubMed: 16179945]
27. Si Y, Shi H, Lee K. Metabolic flux analysis of mitochondrial uncoupling in 3T3-L1 adipocytes. PloS one. 2009; 4:e7000. [PubMed: 19746157]
28. Tseng YH, Cypess AM, Kahn CR. Cellular bioenergetics as a target for obesity therapy. Nat Rev Drug Discov. 2010; 9:465–482. [PubMed: 20514071]
29. Harper JA, Dickinson K, Brand MD. Mitochondrial uncoupling as a target for drug development for the treatment of obesity. Obes Rev. 2001; 2:255–265. [PubMed: 12119996]
30. Harper ME, Green K, Brand MD. The efficiency of cellular energy transduction and its implications for obesity. Annu Rev Nutr. 2008; 28:13–33. [PubMed: 18407744]
31. Clapham JC, et al. Mice overexpressing human uncoupling protein-3 in skeletal muscle are hyperphagic and lean. Nature. 2000; 406:415–418. [PubMed: 10935638]
32. Kopecky J, Clarke G, Enerback S, Spiegelman B, Kozak LP. Expression of the mitochondrial uncoupling protein gene from the aP2 gene promoter prevents genetic obesity. J Clin Invest. 1995; 96:2914–2923. [PubMed: 8675663]
33. Li B, et al. Skeletal muscle respiratory uncoupling prevents diet-induced obesity and insulin resistance in mice. Nature medicine. 2000; 6:1115–1120.
34. Neschen S, et al. Uncoupling protein 1 expression in murine skeletal muscle increases AMPK activation, glucose turnover, and insulin sensitivity in vivo. Physiol Genomics. 2008; 33:333–340. [PubMed: 18349383]
35. Ishigaki Y, et al. Dissipating excess energy stored in the liver is a potential treatment strategy for diabetes associated with obesity. Diabetes. 2005; 54:322–332. [PubMed: 15677488]
36. Choi CS, et al. Overexpression of uncoupling protein 3 in skeletal muscle protects against fat-induced insulin resistance. The Journal of clinical investigation. 2007; 117:1995–2003. [PubMed: 17571165]
37. Amara CE, et al. Mild mitochondrial uncoupling impacts cellular aging in human muscles in vivo. Proc Natl Acad Sci U S A. 2007; 104:1057–1062. [PubMed: 17215370]
38. Maragos WF, Korde AS. Mitochondrial uncoupling as a potential therapeutic target in acute central nervous system injury. J Neurochem. 2004; 91:257–262. [PubMed: 15447659]
39. Mattiasson G, et al. Uncoupling protein-2 prevents neuronal death and diminishes brain dysfunction after stroke and brain trauma. Nature medicine. 2003; 9:1062–1068.
40. Parascandola J. Dinitrophenol and bioenergetics: an historical perspective. Molecular and cellular biochemistry. 1974; 5:69–77. [PubMed: 4610359]
41. Perry RJ, et al. Reversal of hypertriglyceridemia, fatty liver disease, and insulin resistance by a liver-targeted mitochondrial uncoupler. Cell Metab. 2013; 18:740–748. [PubMed: 24206666]
42. Frayha GJ, Smyth JD, Gobert JG, Savel J. The mechanisms of action of antiprotozoal and anthelmintic drugs in man. Gen Pharmacol. 1997; 28:273–299. [PubMed: 9013207]
43. Sheth UK. Mechanisms of anthelmintic action. Prog Drug Res. 1975; 19:147–157. [PubMed: 769059]
44. Weinbach EC, Garbus J. Mechanism of action of reagents that uncouple oxidative phosphorylation. Nature. 1969; 221:1016–1018. [PubMed: 4180173]

Author Manuscript Author Manuscript Author Manuscript Author Manuscript

45. Andrews P, Thyssen J, Lorke D. The Biology and Toxicology of Molluscidides, Bayluscide. Pharmc. Ther. 1983; 19:245–295.
46. Hecht G, Gloxhuber C. Tolerance to 2′, 5-dichloro-4-nitrosalicylanilide ethanolamine salt. Z. Tropenmed. Parasit. 1962; 13:1–8.
47. Owen MR, Doran E, Halestrap AP. Evidence that metformin exerts its anti-diabetic effects through inhibition of complex 1 of the mitochondrial respiratory chain. Biochem J. 2000; 348(Pt 3):607–614. [PubMed: 10839993]
48. Misbin RI, et al. Lactic acidosis in patients with diabetes treated with metformin. N Engl J Med. 1998; 338:265–266. [PubMed: 9441244]
49. Kobayashi K, et al. The db/db mouse, a model for diabetic dyslipidemia: molecular characterization and effects of Western diet feeding. Metabolism: clinical and experimental. 2000; 49:22–31. [PubMed: 10647060]
50. Samuel VT, et al. Mechanism of hepatic insulin resistance in non-alcoholic fatty liver disease. The Journal of biological chemistry. 2004; 279:32345–32353. [PubMed: 15166226]
51. Fryer LG, Parbu-Patel A, Carling D. The Anti-diabetic drugs rosiglitazone and metformin stimulate AMP-activated protein kinase through distinct signaling pathways. J Biol Chem. 2002; 277:25226–25232. [PubMed: 11994296]
52. Inoki K, Zhu T, Guan KL. TSC2 mediates cellular energy response to control cell growth and survival. Cell. 2003; 115:577–590. [PubMed: 14651849]
53. Zhou G, et al. Role of AMP-activated protein kinase in mechanism of metformin action. The Journal of clinical investigation. 2001; 108:1167–1174. [PubMed: 11602624]
54. Chen M, et al. The anti-helminthic niclosamide inhibits Wnt/Frizzled1 signaling. Biochemistry. 2009; 48:10267–10274. [PubMed: 19772353]
55. Osada T, et al. Antihelminth compound niclosamide downregulates Wnt signaling and elicits antitumor responses in tumors with activating APC mutations. Cancer research. 2011; 71:4172–4182. [PubMed: 21531761]
56. Sack U, et al. Novel effect of antihelminthic Niclosamide on S100A4-mediated metastatic progression in colon cancer. J Natl Cancer Inst. 2011; 103:1018–1036. [PubMed: 21685359]
57. Ren X, et al. Identification of Niclosamide as a New Small-Molecule Inhibitor of the STAT3 Signaling Pathway. ACS Med. Chem. Lett. 2010; 1:454–459. [PubMed: 24900231]
58. Madiraju AK, et al. Metformin suppresses gluconeogenesis by inhibiting mitochondrial glycerophosphate dehydrogenase. Nature. 2014; 510:542–546. [PubMed: 24847880]
59. Krieger R, Krieger W. Handbook of pesticide toxicology. 2001:1225–1247.
60. Swan GE. The pharmacology of halogenated salicylanilides and their anthelmintic use in animals. J S Afr Vet Assoc. 1999; 70:61–70. [PubMed: 10855824]
61. Frezza C, Cipolat S, Scorrano L. Organelle isolation: functional mitochondria from mouse liver, muscle and cultured fibroblasts. Nat Protoc. 2007; 2:287–295. [PubMed: 17406588]
62. Trounce IA, Kim YL, Jun AS, Wallace DC. Assessment of mitochondrial oxidative phosphorylation in patient muscle biopsies, lymphoblasts, and transmitochondrial cell lines. Methods Enzymol. 1996; 264:484–509. [PubMed: 8965721]
63. Muoio DM, Seefeld K, Witters LA, Coleman RA. AMP-activated kinase reciprocally regulates triacylglycerol synthesis and fatty acid oxidation in liver and muscle: evidence that sn-glycerol-3-phosphate acyltransferase is a novel target. Biochem J. 1999; 338(Pt 3):783–791. [PubMed: 10051453]
64. Zhang Y, et al. Adipose-specific deletion of autophagy-related gene 7 (atg7) in mice reveals a role in adipogenesis. Proc Natl Acad Sci U S A. 2009; 106:19860–19865. [PubMed: 19910529]
65. Prince A, Zhang Y, Croniger C, Puchowicz M. Oxidative metabolism: glucose versus ketones. Advances in experimental medicine and biology. 2013; 789:323–328. [PubMed: 23852511]
66. Chang Y-W, et al. Pharmacokinetics of Anti-SARS-CoV Agent Niclosamide and Its Analogs in Rats. Journal of Food and Drug Analysis. 2006; 14:329–333.
67. Kim HJ, et al. Differential effects of interleukin-6 and -10 on skeletal muscle and liver insulin action in vivo. Diabetes. 2004; 53:1060–1067. [PubMed: 15047622]

Author Manuscript Author Manuscript Author Manuscript Author Manuscript

68. Yu CL, et al. Mechanism by which fatty acids inhibit insulin activation of insulin receptor substrate-1 (IRS-1)-associated phosphatidylinositol 3-kinase activity in muscle. Journal of Biological Chemistry. 2002; 277:50230–50236. [PubMed: 12006582]

Author Manuscript Author Manuscript Author Manuscript Author Manuscript

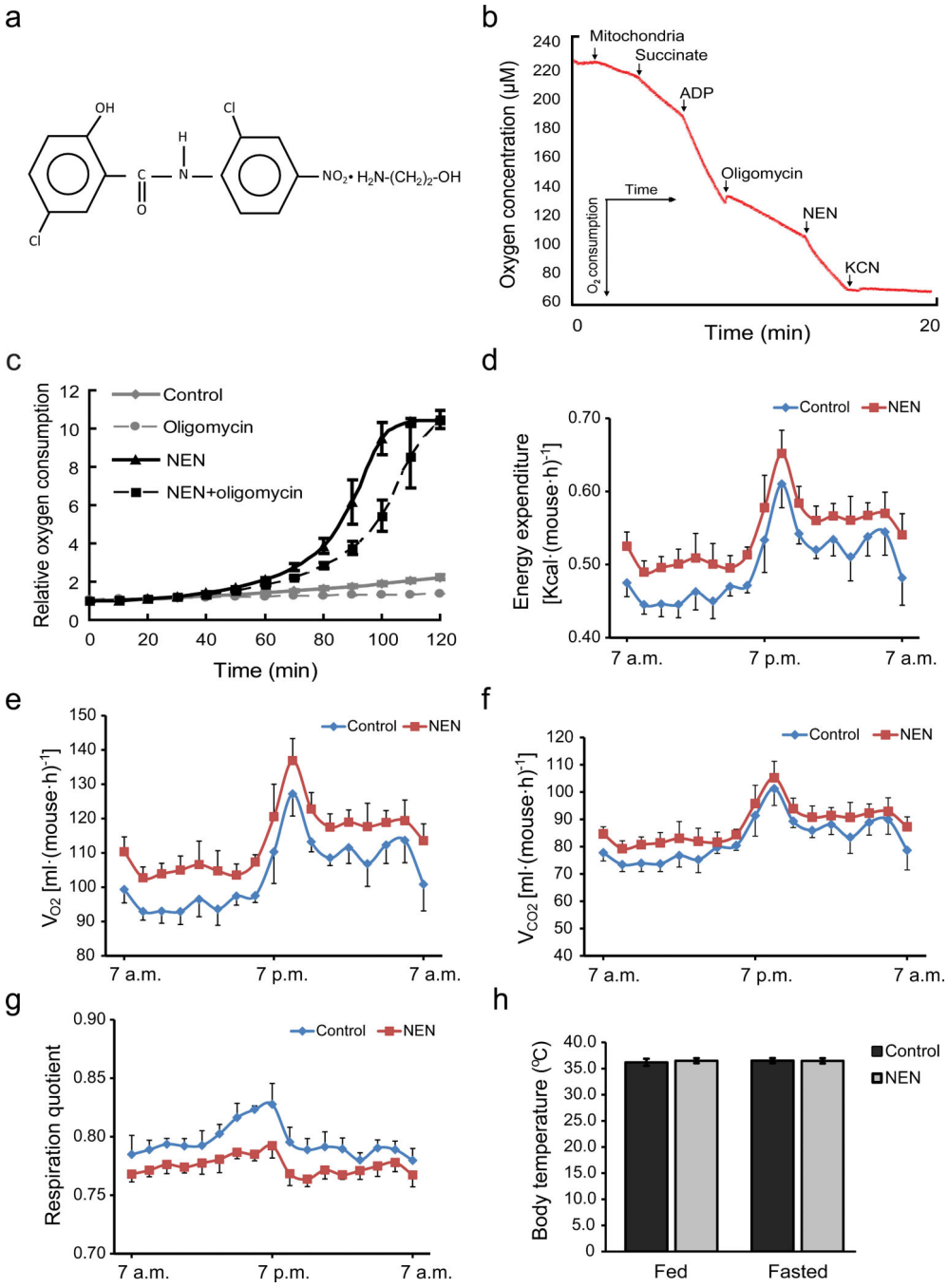

Figure 1.

NEN uncouples mitochondrial respiration and impacts on mouse energy metabolism. (**a**) Chemical structure of niclosamide ethanolamine salt (NEN, 5-chloro-salicyl-(2-chloro-4-nitro) anilide 2-aminoethanol salt). (**b**) Oxygen consumption assay of isolated mouse liver mitochondria, showing oxygen concentration continuously measured as the indicated respiration substrates and inhibitors added into the respiration system to the final concentrations: succinate, 5 mM; ADP, 125 nM; oligomycin, 5 μg·ml^{-1}, NEN, 1 μM; KCN, 2 mM. (**c**) Cellular oxygen consumption assay of NIH-3T3 cells treated with vehicle

Author Manuscript Author Manuscript Author Manuscript Author Manuscript

(Control), 1 μM NEN (NEN), 5 $\mu g \cdot ml^{-1}$ oligomycin (Oligomycin), or both (NEN + oligomycin). (**d**) Mouse energy expenditure, *p=0.01*. (**e**) Mouse oxygen consumption (V_{O2}), *p<0.01*. (**f**) Mouse carbon dioxide generation (V_{CO2}), *p=0.05*. (**g**) Mouse respiration quotient, $p < 0.001$. (**h**) Mouse rectal temperature. For **d**, **e**, **f**, **g** and **h**, male C57BL/6 mice were fed with HFD (control) or same HFD with 1,500 ppm NEN (NEN) for 1 wk, $n = 8$ for all groups. Statistical test in **d**, **e**, **f** and **g**, one-way analysis of variance (ANOVA); in **h**, student t-test.

Author Manuscript Author Manuscript Author Manuscript Author Manuscript

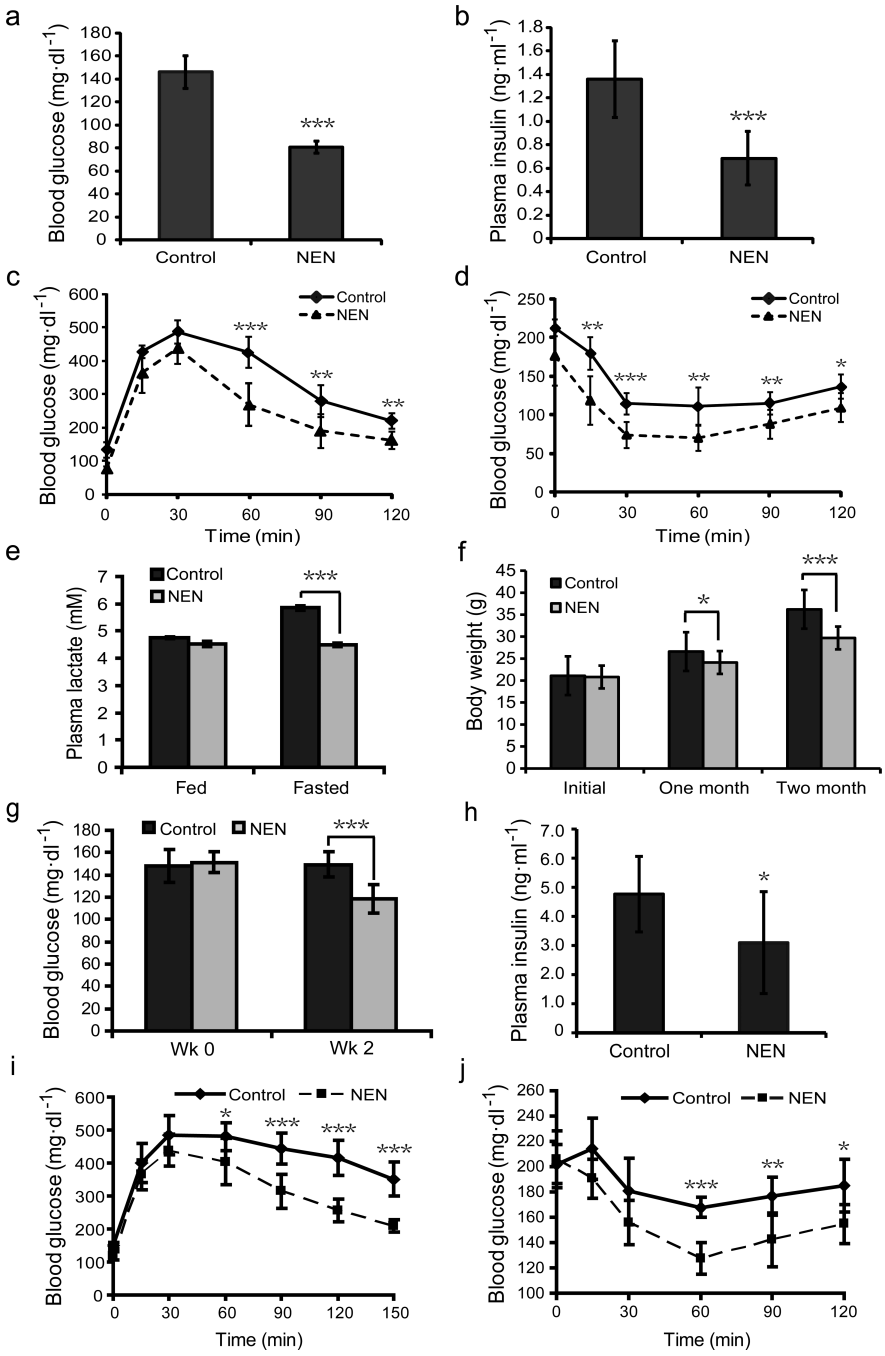

Figure 2.

Oral NEN is effective in preventing and treating HFD-induced insulin resistance. (**a**) Fasting blood glucose concentration of male C57BL/6 mice fed with either HFD (Control) or HFD with 1,500 ppm NEN (NEN), measured at wk 8 on HFD diet. (**b**) Basal plasma insulin concentration of the mice, as defined in **a**, measured at wk 8. (**c**) Glucose tolerance assay, and (**d**) insulin sensitivity assay of the mice, as defined in **a**, performed at wk 10. (**e**) Plasma lactate concentration of the mice, as defined in **a**, measured at wk 16 under indicated conditions. (**f**) Body weight of the mice, as defined in **a**, measured at indicated time points.

Author Manuscript Author Manuscript Author Manuscript Author Manuscript

(**g**) Fasting blood glucose concentration of male C57BL/6J mice that were first fed with HFD for 16 wk, and then randomized into two groups fed either with HFD (Control), or HFD containing 1,500 ppm NEN (NEN). The time when NEN containing food was initiated is designated as wk 0. (**h**) Basal plasma insulin concentration of the mice, as defined in **g**, measured at wk 2. (**i**) Glucose tolerance assay, and (**j**) insulin sensitivity assay of the mice, as defined in **g**, performed at wk 3. $n = 7$ for all groups. Student t-test, $^{*}P < 0.05$; $^{**}P < 0.01$; $^{***}P < 0.001$; error bar, s.d.

Author Manuscript Author Manuscript Author Manuscript Author Manuscript

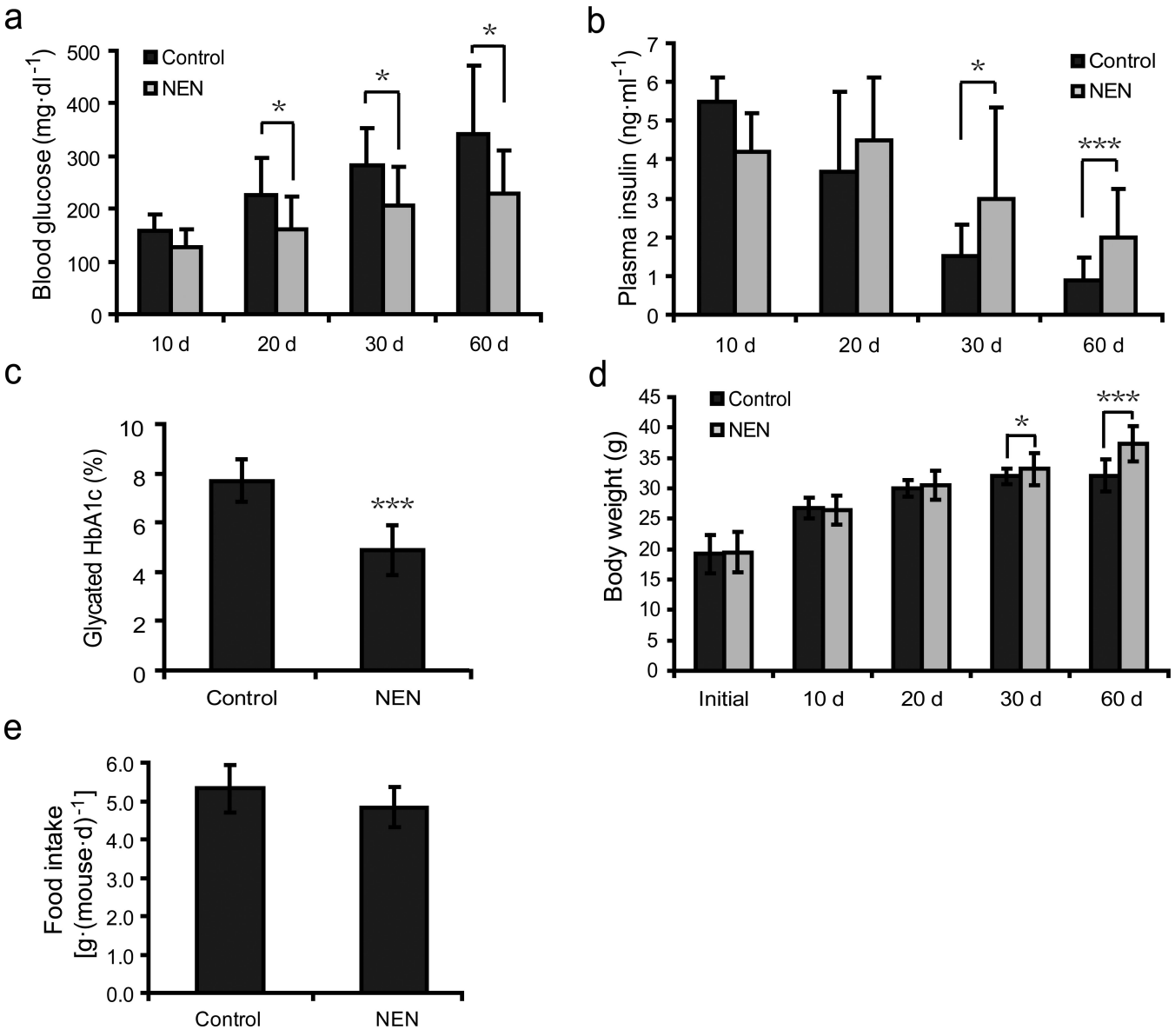

Figure 3.

Oral NEN improves glycemic control in *db/db* mice. (**a**) Fasting blood glucose concentration of *db/db* mice fed with either normal chow diet (control), or the same chow diet containing 1,500 ppm NEN (NEN), measured at indicated time points. (**b**) Basal plasma insulin concentration of the *db/db* mice as defined in **a**, measured at indicated time points. (**c**) Glycated hemoglobin A1c (HbA1c) level of the *db/db* mice as defined in **a**, measured at day 60. (**d**) Body weight of the *db/db* mice as defined in **a**, measured at indicated time points. (**e**) Daily food intake of the *db/db* mice as defined in **a**. $n = 9$ for all groups. Student t-test; *$P <$ 0.05; ***$P < 0.001$; error bar, s.d.

Author Manuscript Author Manuscript Author Manuscript Author Manuscript

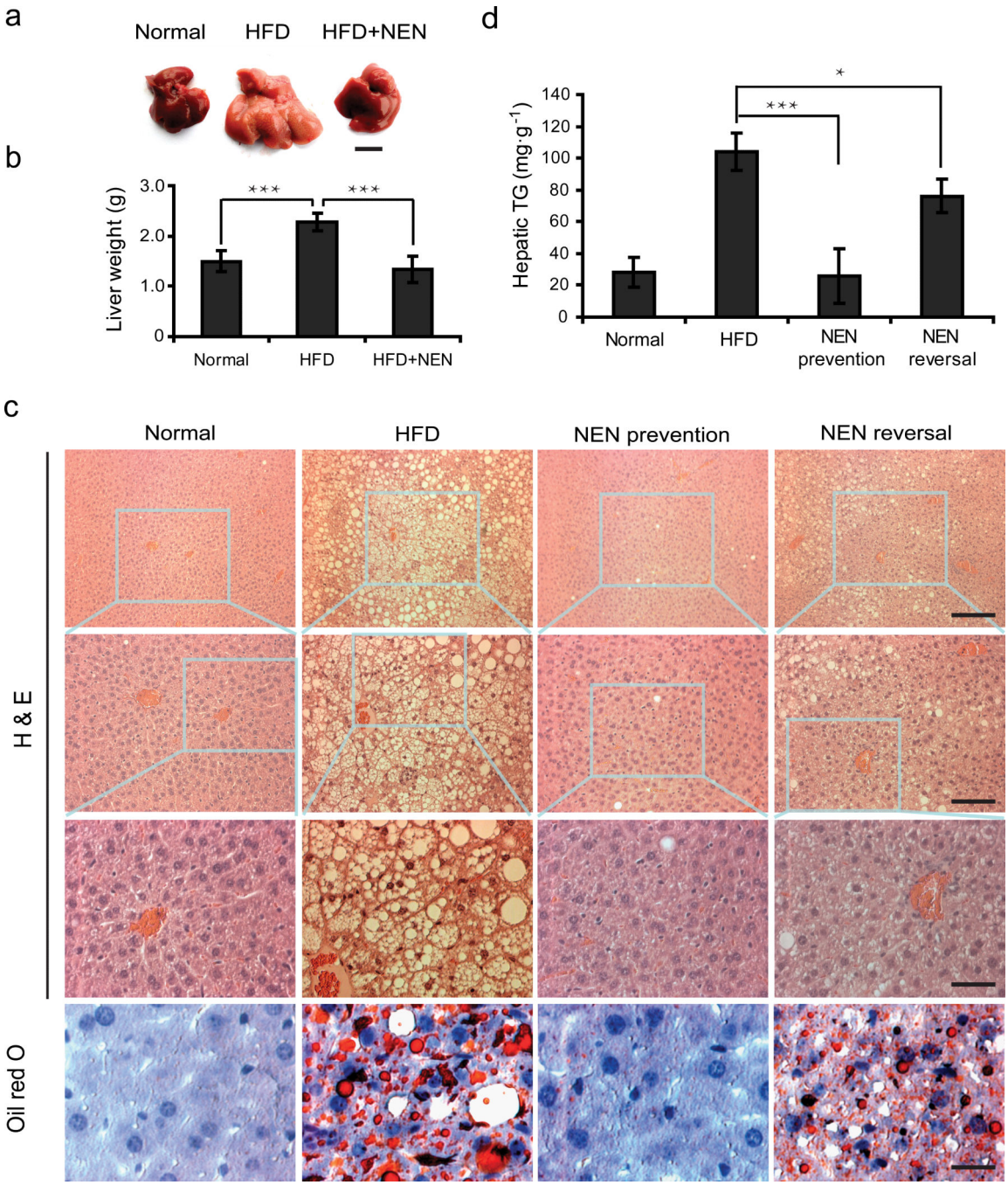

Figure 4.

Oral NEN is effective in preventing and reducing HFD- induced hepatic steatosis in mice. (**a**) Representative liver morphology; scale bar, 1 cm; and (**b**) weight of whole liver of male C57BL/6J mice fed with normal chow diet (Normal), or HFD (HFD), or HFD containing 1,500 ppm NEN (HFD+NEN) for 16 wk starting at 5 wk of age, $n = 3$. (**c**) Representative liver sections stained with hematoxylin and eosin (H & E) or with Oil Red O, as indicated, and (**d**) quantification of hepatic triglyceride content, normalized to tissue weight, of liver tissue samples from male C57BL/6J mice fed for 16 wk with normal chow diet (Normal), or

Author Manuscript Author Manuscript Author Manuscript Author Manuscript

HFD, or HFD containing 1,500 ppm NEN (NEN prevention), or first fed with HFD for 16 wk and then switched to HFD containing 1,500 ppm NEN for 4 wk (NEN reversal). For **c** and **d**, $n = 7$ for all groups; in H & E staining of **c**, upper panel scale bar, 200 μm; middle panel scale bar, 100 μm; lower panel scale bar, 50 μm; for Oil Red O staining sections, scale bar, 50 μm. Student t-test, $*P < 0.05$; $***P < 0.001$, error bar, s.d.

Author Manuscript Author Manuscript Author Manuscript Author Manuscript

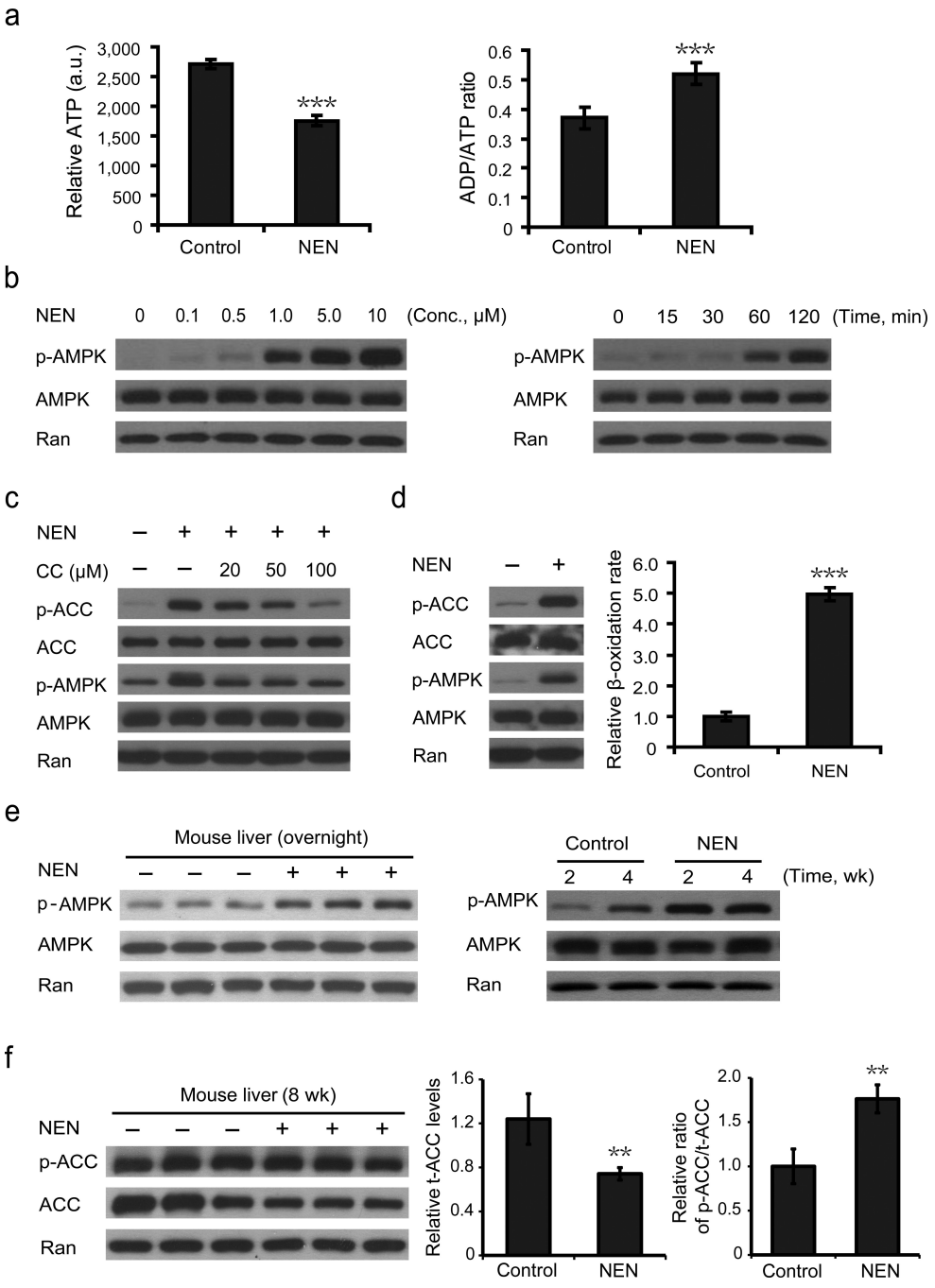

Figure 5.

Effect of NEN on cellular metabolism. (**a**) Relative intracellular ATP concentrations (left panel) and ADP/ATP ratio (right panel) in cultured HepG2 cells without NEN treatment (control) or treated with 1.0 μM NEN for 2 h (NEN). (**b**) Immunoblotting analyses of NIH-3T3 cells showing NEN activates AMPK in a dose- (left panel, 2 h, indicated concentrations of NEN) and time- (right panel, 1.0 μM NEN, indicated time points) dependent manner. (**c**) Immunoblotting analyses of the phosphorylation of AMPK and ACC in NIH-3T3 cells without treatment, or treated with 1.0 μM NEN alone, or treated with NEN

Author Manuscript Author Manuscript Author Manuscript Author Manuscript

in combination with AMPK inhibitor Compound C (CC) at indicated concentrations for 2 h. (**d**) Immunoblotting analyses of the phosphorylation of AMPK and ACC (left panel) and β-oxidation analyses (right panel) of HepG2 cells treated with or without 1.0 μM NEN for 2 h. (**e**) Immunoblotting analyses of AMPK phosphorylation in mouse liver from male C57BL/6J mice either fed with HFD (control) or HFD containing 1,500 ppm NEN (NEN) for overnight (left panel), or indicated period of time (right panel). (**f**) Immunoblotting analyses (left panel) and the quantifications (middle and right panels) of the expression and phosphorylation of ACC in liver samples from micefed for 8 wk HFD with or without NEN. p-AMPK, phosphorylated AMPK (Thr172); p-ACC, phosphorylated ACC (Ser79). Student t-test, $^{**}P < 0.01$; $^{***}P < 0.001$, error bar, s.d.

Author Manuscript Author Manuscript Author Manuscript Author Manuscript

Table 1

Hyperinsulinemic-euglycemic clamp study

Treat	Basal glucose ($mg \cdot dl^{-1}$)	Clamp glucose ($mg \cdot dl^{-1}$)	Glucose infusion rate $[mg \cdot (kg \cdot min)^{-1}]$	Glucose turnover $[mg \cdot (kg \cdot min)^{-1}]$	Basal HGP $[mg \cdot (kg \cdot min)^{-1}]$	Clamp HGP $[mg \cdot (kg \cdot min)^{-1}]$	Hepatic insulin action (%)	Whole Body glycolysis $[mg \cdot (kg \cdot min)^{-1}]$	Glycogen synthesis $[mg \cdot (kg \cdot min)^{-1}]$
Control (n=11)	**159±6**	**121±2**	**29.6±2.6**	**40.3±2.5**	**13.9±0.9**	**10.7±1.6**	**28.7±9.5**	**30.8±2.5**	**9.5±1.0**
NEN (n=11)	**140±7**	**121±4**	**43.0±3.0**	**48.7±3.0**	**15.4±1.6**	**5.7±2.0**	**61.5±10.0**	**31.5±1.7**	**17.2±2.2**
p-value[a]	**0.043**	**0.943**	**0.003**	**0.045**	**0.408**	**0.065**	**0.027**	**0.814**	**0.005**

Data are expressed as means ± s.d.

[a] Student t-test.